# 25

# Geotechnical Earthquake Engineering




Jonathan D. Bray
*University of California at Berkeley*


## 25.1 Introduction

Geotechnical factors often exert a major influence on damage patterns and loss of life in earthquake events. For example, the localized patterns of heavy damage during the 1985 Mexico City and 1989 Loma Prieta, California, earthquakes provide grave illustrations of the importance of understanding the seismic response of deep clay deposits and loose, saturated sand deposits. The near failure of the Lower San Fernando dam in 1971 due to liquefaction of the upstream shell materials is another grave reminder that we must strive to understand the seismic response of critical earth structures. The characteristics and distribution of earth materials at a project site significantly influence the characteristics of the earthquake ground motions, and hence significantly influence the seismic response of the constructed facilities at a site. Moreover, the composition and geometry of earth structures, such as earth dams and solid waste landfills, significantly affect their seismic response. Geotechnical considerations therefore play an integral role in the development of sound earthquake-resistant designs. In this chapter, geotechnical earthquake engineering phenomena such as site-specific amplification, soil liquefaction, and seismic slope stability are discussed. Case histories are used to illustrate how earthquakes affect engineered systems, and established, simplified empirical procedures that assist engineers in assessing the effects of these phenomena are presented. The field of earthquake engineering is quite complex, so the need for exercising engineering judgment based on appropriate experience is emphasized.

## 25.2 Earthquake Strong Shaking

The development and transmission of earthquake energy through the underlying geology is quite complex, and a site-specific seismic response study requires an assessment of the primary factors influencing the ground motion characteristics at a site. They are

- Earthquake source mechanism
- Travel path geology

- Topographic effects
- Earthquake magnitude
- Distance from zone of energy release
- Local soil conditions

Earthquakes are produced in a particular geologic setting due to specific physical processes. A midplate earthquake (e.g., New Madrid) will differ from a plate margin earthquake (e.g., San Andreas) [see Nuttli, 1982]. The principal descriptive qualities of the earthquake source are the type of fault displacement (strike-slip, normal, or reverse), depth of the rupture, length of the rupture, and duration of the rupturing. The characteristics of the rock which the seismic waves travel through influence the frequency content of the seismic energy. Significant topographic features (e.g., basins) can focus and hence amplify earthquake motions. The **magnitude** of an earthquake is related to the amount of energy released during the event. The difference between earthquakes of different magnitudes is significant; for example, a magnitude 7 earthquake event releases nearly a thousand times more energy than a magnitude 5 event. The potential for seismic damage will typically increase with earthquake events of greater magnitude. Seismic energy attenuates as it travels away from the zone of energy release and spreads out over a greater volume of material. Hence, the intensity of the bedrock motion will typically decrease as the distance of a particular site from the zone of energy release increases. A number of **attenuation relationships** based on earthquake magnitude and distance from the earthquake fault rupture are available [e.g., Nuttli and Herrmann, 1984; Joyner and Boore, 1988; Idriss, 1991]. Local soil conditions may significantly amplify ground shaking, and some soil deposits may undergo severe strength loss resulting in ground failure during earthquake shaking. The last three factors listed above (magnitude, distance, local soil conditions) are usually the most important factors, and most seismic studies focus on these factors.

There are several earthquake magnitude scales, so it is important to use these scales consistently. The earliest magnitude scale, local magnitude ($M_L$), was developed by Richter [1935] and is defined as the logarithm of the maximum amplitude on a Wood-Anderson torsion seismogram located at a distance of 100 km from the earthquake source [Richter, 1958]. Other related magnitude scales include surface wave magnitude, $M_s$, and body wave magnitudes, $m_b$ and $m_B$ [Gutenberg and Richter, 1956]. These magnitude scales are based on measurement of the amplitude of the seismic wave at different periods ($M_L$ at 0.8 s, $m_b$ and $m_B$ between 1 s and 5 s, and $M_s$ at 20 s), and hence they are not equivalent. The moment magnitude, $M_w$, is different from these other magnitude scales because it is directly related to the dimensions and characteristics of the fault rupture. Moment magnitude is defined as

$$M_w = \frac{2}{3} \log M_0 - 10.7 \tag{25.1}$$

where $M_0$ is the seismic moment in dyne-cm, with $M_0 = \mu \cdot A_f \cdot D$; $\mu$ = shear modulus of material along the fault plane (typically $3 \times 10^{11}$ dyne/cm$^2$), $A_f$ = area of fault rupture in cm$^2$, and $D$ = average slip over the fault rupture in cm [Hanks and Kanamori, 1979]. Heaton et al. [1982] has shown that these magnitude scales are roughly equivalent up to $M_w = 6$, but that magnitude scales other than $M_w$ reach limiting values for higher moment magnitude earthquake events (i.e., max $m_b \approx 6$, max $M_L \approx 7$, max $m_B \approx 7.5$, and max $M_s \approx 8$). Thus, the use of moment magnitude is preferred, but the engineer must use the appropriate magnitude scale in available correlations between engineering parameters and earthquake magnitude.

The earthquake motion characteristics of engineering importance are

- Intensity
- Frequency content
- Duration

The intensity of ground shaking is usually portrayed by the **maximum horizontal ground acceleration (MHA)**, but since velocity is a better indicator of the earthquake energy that must be dissipated by an engineered system, it should be used as well. The MHA developed from a site-specific seismicity study

| Geologic and Seismologic Evaluation | Geotechnical Evaluation | Structural Design |
|---|---|---|
| • Identify Seismic Sources | • Site Response | • Dynamic Analysis |
| • Potential for Surface Rupture | • Liquefaction Potential | - Pseudo-static |
| • Size and Frequency of Events | • Seismic Stability | - Time History |
| • Develop Rock Motions | • Soil-Structure Interaction | • Design Considerations |

**FIGURE 25.1** Seismic hazard assessment.

should be compared to that presented in the U.S. Geological Survey maps prepared by Algermissen et al. [1991] and the seismic zone factor ($Z$) given in the Uniform Building Code. The frequency content of the ground motions is typically characterized by its **predominant period ($\mathbf{T_p}$)**. The predominant period of the ground motions at a site tends to increase with higher magnitude events and with greater distances from the zone of energy release [see Idriss, 1991]. Earthquake rock motions with a concentration of energy near the fundamental periods of the overlying soil deposit and structure have a greater potential for producing amplified shaking and seismic damage. Lastly, the **duration of strong shaking** is related to the earthquake's magnitude and is typically described by the duration of the earthquake record in which the intensity is sufficiently high to be of engineering importance (i.e., MHA exceeding around 0.05$g$) or the equivalent number of cycles of strong shaking [see Seed and Idriss, 1982].

A seismic hazard assessment generally involves those items listed in Fig. 25.1. Earthquake engineering is a multidisciplinary field that requires a coordinated effort. The success of the geotechnical evaluation depends greatly on the results of the geological and seismological evaluation, and the results of the geotechnical evaluation must be compatible with the requirements of the structural design.

## 25.3 Site-Specific Amplification

The localized patterns of heavy damage during the 1989 Loma Prieta earthquake in northern California demonstrate the importance of understanding the seismic response of deep soil deposits. Well over half of the economic damage and more than 80% of the loss of life occurred on considerably less than 1% of the land within 80 km of the fault rupture zone largely as a result of site-specific effects [Seed et al., 1990]. For example, in the Oakland area, which is 70 km away from the rupture zone, maximum horizontal ground accelerations were amplified by a factor of 2 to 4 and spectral accelerations at some frequencies were amplified by a factor of 3 to 8 [Bray et al., 1992]. The dramatic collapse of the elevated highway I-880 structure, in which 38 people died, is attributed in part to these amplified strong motions [Hough et al., 1990]. Hundreds of buildings in the San Francisco Bay area sustained significant damage because of earthquake strong shaking. These observations are critical to many cities as deep soil deposits exist in many earthquake-prone areas around the world. For example, records of the January 31, 1986 northeastern Ohio earthquake suggest that similar site-specific amplification effects could occur in the central U.S. and produce heavy damage during a major event in the New Madrid seismic zone [Nuttli, 1987].

Response spectra are typically used to portray the characteristics of the earthquake shaking at a site. The **response spectrum** shows the maximum response induced by the ground motions in damped single-degree-of-freedom structures of different **fundamental periods**. Each structure has a unique fundamental period at which the structure tends to vibrate when it is allowed to vibrate freely without any external excitation. The response spectrum indicates how a particular structure with its inherent fundamental period would respond to the earthquake ground motion. For example, referring to Fig. 25.2, a low-period structure (say, $T = 0.1$ s) at the SCT building site would experience a maximum acceleration of 0.14$g$, whereas a higher-period structure (say, $T = 2.0$ s) at the SCT site would experience a maximum acceleration of 0.74$g$ for the same ground motions.

The response spectra shown in Fig. 25.2 illustrate the pronounced influence of local soil conditions on the characteristics of the observed earthquake ground motions. Since Mexico City was located approximately 400 km away from the earthquake's epicenter, the observed response at rock and hard soil sites

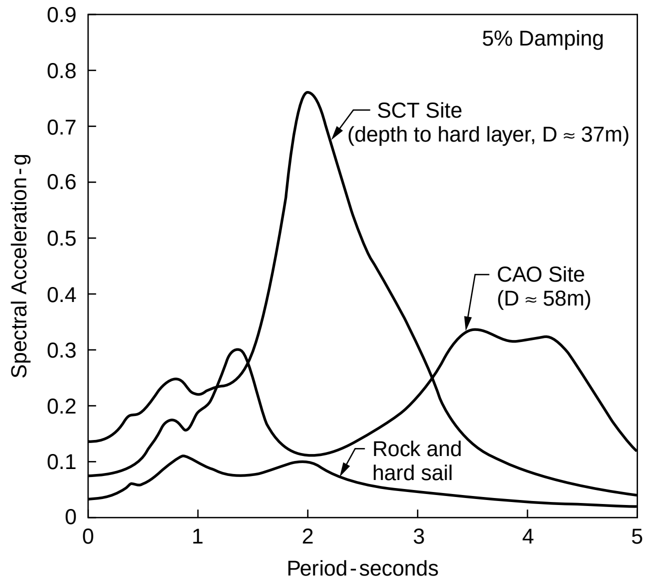


**FIGURE 25.2** Acceleration response spectra for motions recorded in Mexico City during the 1985 Mexico City earthquake (after Seed, H. B., Romo, M. P., Sun, J., Jaime, A., and Lysmer, J. 1987. Relationships between Soil Conditions and Earthquake Ground Motions in Mexico City in the Earthquake of Sept. 19, 1985. Earthquake Engineering Research Center, Report No. UCB/EERC-87/15, University of California, Berkeley).

was fairly low (i.e., the spectral accelerations were less than 0.1*g* at all periods). Damage was correspondingly negligible at these sites. At the Central Market site (CAO), spectral accelerations were significantly amplified at periods of around 1.3 s and within the range of 3.5 s to 4.5 s. Since buildings at the CAO site did not generally have fundamental periods within these ranges, damage was fairly minor. The motion recorded at the SCT building site, however, indicated significant amplification of the underlying bedrock motions with a maximum horizontal ground acceleration (the spectral acceleration at a period of zero) over four times that of the rock and hard soil sites and with a spectral acceleration at $T = 2.0$ s over seven times that of the rock and hard soil sites. Major damage, including collapse, occurred to structures with fundamental periods ranging from about 1 s to 2 s near the SCT building site and in areas with similar subsurface conditions. At these locations, the soil deposit's fundamental period *matched* that of the overlying structures, creating a resonance condition that amplified strong shaking and caused heavy damage.

The 1991 Uniform Building Code (UBC) utilizes site coefficients in its pseudostatic design base shear procedure to limit damage due to local soil conditions (see Table 25.1). For example, the site coefficient for soil characteristics ($S$ factor) is increased to 2.0 for the soft soil profile $S_4$, and an $S$ factor of 1.0 is used at rock sites where no soil-induced amplification occurs. However, a deposit of stiff clay greater than 61 m thick, such as those that underlay Oakland, would be categorized as soil profile $S_2$ with an $S$ factor of only 1.2. The seismic response of the deep stiff clay sites during the 1989 Loma Prieta earthquake with spectral amplification factors on the order of 3 to 8 suggest that we may be currently underestimating the seismic hazard at these sites. Earthquake engineering is a relatively young field of study, and additional research is required to support the evolution of safer building codes.

The UBC also allows dynamic analyses of structural systems and provides the normalized response spectra shown in Fig. 25.3. The spectral acceleration of a structure can be estimated from this figure given an estimate of the system's fundamental period ($T$), the peak ground acceleration (MHA) of the design event, and the classification of the subsurface soil conditions. At longer periods ($T > 0.5$ s), the spectral accelerations for deep soil sites (soil type 2) and soft soil sites (soil type 3) are significantly higher than that for rock and stiff soils (soil type 1). The engineer can also use wave propagation analyses [e.g., SHAKE91; see Idriss and Sun, 1992] to develop a site-specific design response spectrum based on the

**TABLE 25.1** 1991 UBC Site Coefficients[a,b]

| Type | Description | $S$ factor |
|---|---|---|
| $S_1$ | A soil profile with either (a) a rock-like material characterized by a shear wave velocity greater than 762 mps or by other suitable means of classification, or (b) stiff or dense soil condition where the soil depth is less than 61 m | 1.0 |
| $S_2$ | A soil profile with dense or stiff soil conditions where the soil depth exceeds 61 m | 1.2 |
| $S_3$ | A soil profile 21 m or more in depth and containing more than 6 m of soft to medium stiff clay but not more than 12 m of soft clay | 1.5 |
| $S_4$ | A soil profile containing more than 12 m of soft clay characterized by a shear wave velocity less than 152 mps | 2.0 |

[a] The site factor shall be established from properly substantiated geotechnical data. In location where the soil properties are not known in sufficient detail to determine the soil profile type, soil profile $S_1$ shall be used. Soil profile $S_4$ need not be assumed unless the building official determines that soil profile $S_4$ may be present at the site, or in the event soil profile $S_4$ is established by geotechnical data.

[b] The total design base shear ($V$) is determined from the formula $V = Z \cdot I \cdot C \cdot W/R_w$, where $C = 1.225S/T^{2/3} \leq 2.75$. $Z$ = seismic zone factor, $I$ = importance factor, $S$ = site coefficient, $T$ = fundamental period of structure, $W$ = total seismic dead load, and $R_w$ = reduction coefficient based on the lateral load-resisting system (see UBC). Hence $V \propto S$ if $C < 2.75$.

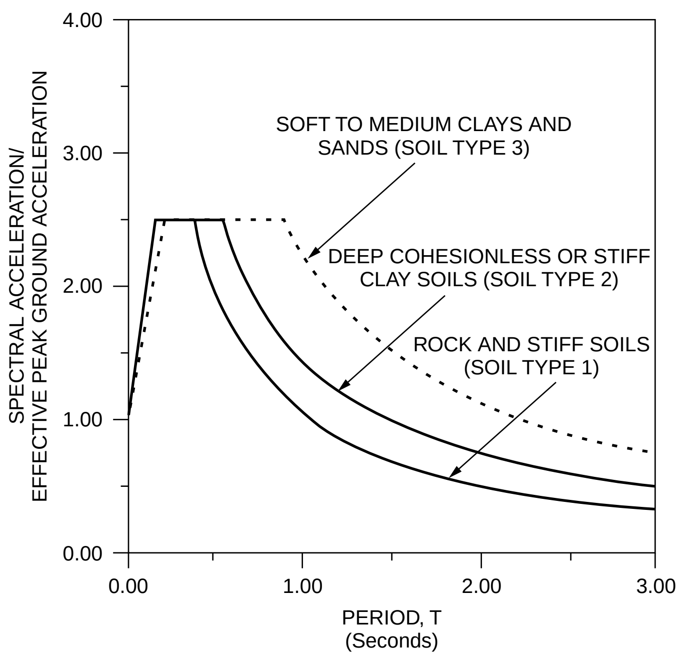


**FIGURE 25.3** 1991 UBC normalized acceleration response spectra.

geologic, seismologic, and soil characteristics associated with the project site. The seismic response of earth materials is dictated primarily by geometric considerations and by the soil's dynamic properties (e.g., shear modulus and damping characteristics). The shear modulus gives an indication of the stiffness of the soil system, whereas the **damping ratio** provides a measure of the soil system's ability to dissipate energy under cyclic loading. Soils exhibit strain-dependent dynamic properties so that as earthquake strong shaking increases and the strain induced in the soil increases, the material's damping ratio increases and its shear modulus decreases [see Seed et al., 1984; Vucetic and Dobry, 1991]. As material damping increases, the soil-induced amplification tends to decrease. As the material stiffness decreases, however, the fundamental period of the soil system increases, and this may affect the amplification of higher-period motions.

The amplification of higher-period ground motions that may match the fundamental period of the building located at the site is one of the most critical concerns in seismic site response studies. If the building's fundamental period is close to that of the site, an earthquake with a concentration of energy around this period would have the potential to produce heavy damage to this structure. The matching of the building and site fundamental periods creates a resonant condition that can amplify shaking. Consideration of a different structural system whose fundamental period does not match that of the underlying soil deposit might be prudent. Otherwise, the design criteria should be more stringent to limit damage to the building during an earthquake event.

## Illustrative Site Response Problem

### Problem 25.1

An eight-story building will be constructed at a deep soil site in Tennessee. As shown in Fig. 25.4, the deep soil site contains surficial deposits of loose, saturated sand overlying a thick clay deposit. The design earthquake is a magnitude ($m_B$) 7.5 event occurring at a distance of 130 km from the site. Develop a preliminary estimate of the maximum horizontal acceleration (MHA) at the site and evaluate the potential for soil-induced amplification of earthquake shaking near the building's fundamental period.

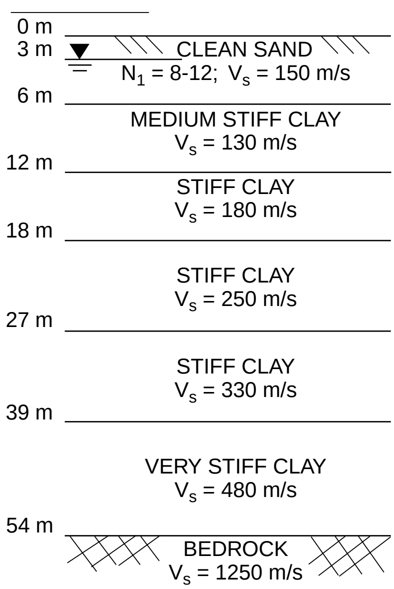


**FIGURE 25.4** Subsurface conditions of project site discussed in Problem 25.1.

#### *Earthquake Strong Shaking*

Limited data is available to develop attenuation curves for the deeper-focus eastern-U.S. earthquakes, and hence this is an area of ongoing research. Nuttli and Herrmann [1984] proposed the attenuation curve shown in Fig. 25.5 for earthquakes likely to occur in the eastern and central U.S. For a site located 130 km from the zone of energy release for an $m_B$ = 7.5 event, the bedrock MHA would be on the order of 0.1*g*. This magnitude of MHA is comparable with what established building codes (e.g., BOCA, SBCCI, and UBC) would recommend for the central part of the state of Tennessee. At this distance (130 km), a magnitude 7.5 earthquake would tend to produce bedrock strong shaking with a predominant period within the range of 0.4 s to 0.7 s [Idriss, 1991].

#### *Site-Specific Amplification*

Comparisons between MHA recorded at deep clay soil sites and those recorded at rock sites indicate that MHA at deep clay soil sites can be 1 to 3 times greater than those at rock sites when $MHA_{rock} \approx 0.1g$ [Bray et al., 1992; Idriss, 1991]. The results of one-dimensional (columnar) dynamic response analyses also suggest MHA amplification factors on the order of 1 to 3 for deep clay sites at low values of $MHA_{rock}$. A proposed relationship between the MHA at soft clay sites and the MHA at rock sites is shown in Fig. 25.6. The estimated rock site MHA value of 0.1*g* would be increased to 0.2*g* for this deep clay site using the average site amplification factor of 2.

The fundamental period of typical buildings can be estimated using the 1991 UBC formula: $T = C_t \cdot (h_n)^{3/4}$, where $T$ = building's fundamental period (s), $C_t$ = structural coefficient = 0.020 for a typical building, and $h_n$ = height of the building (ft). A rough estimate of a level site's fundamental period can be calculated by the formula $T_s = 4D/V_s$, where $T_s$ = the site's fundamental period, $D$ = the soil thickness, and $V_s$ = the soil's average **shear wave velocity**. Computer programs such as SHAKE91 can calculate the site's fundamental period as well as calculate horizontal acceleration and shear stress time histories throughout the soil profile.

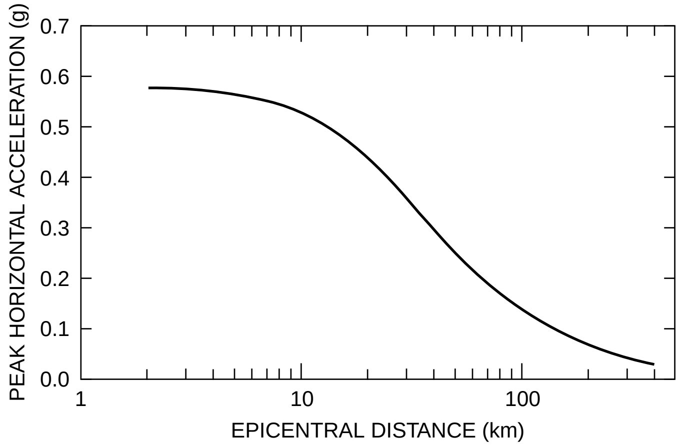


**FIGURE 25.5** MHA attenuation relationship proposed by Nuttli and Herrmann [1984] for $m_B = 7.5$ earthquake in the central U.S.

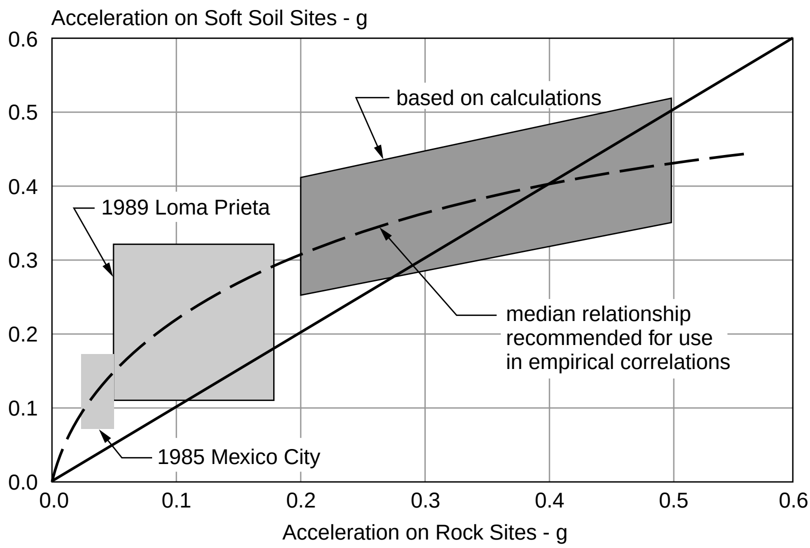


**FIGURE 25.6** Variations of peak horizontal accelerations (MHA) at soft soil sites with accelerations at rock sites (after Idriss, I. M. 1991. Earthquake Ground Motions at Soft Soil Sites. *Proceedings, Second International Conference on Recent Advances in Geotechnical Engineering and Soil Dynamics*, March 11–15, St. Louis, pp. 2265–2272).

Assuming a story height of 13 feet (4 m), the eight-story building would be 104 feet (32 m) high, and $T = 0.020 \cdot (104\ \text{ft})^{3/4} = 0.65$ s. The soil deposit's average initial shear wave velocity is estimated to be $V_s$ = [(150 m/s)(6 m) + (130 m/s)(6 m) + (180 m/s)(6 m) + (250 m/s)(9 m) + (330 m/s)(12 m) + (480 m/s)(15 m)]/54 m = 300 m/s. The site's fundamental period at low levels of shaking is then approximately $T_s = 4 \cdot (54\ \text{m})/300\ \text{m/s} = 0.72$ s. As a check, SHAKE91 analyses calculate the site's fundamental period to be 0.71 seconds, which is in close agreement with the first estimate ($T_s = 0.72$ s).

Since the building's fundamental period ($T = 0.65$ s) is close to that of the site ($T_s = 0.72$ s), an earthquake with a concentration of energy around 0.6 to 0.7 s would have the potential to produce heavy damage to this structure. In fact, SHAKE91 results indicate a maximum spectral acceleration amplification factor of almost 15 at a period around 0.7 s. In comparison, this site would be classified as an $S_3$ site with a site coefficient (or site amplification factor) of 1.5, and the design base shear would be multiplied by an amplification factor of $C = 2.5$ for this site (see Table 25.1). Alternatively, using the normalized response spectrum for deep stiff clay soils in the UBC (Fig. 25.3), the spectral response at $T = 0.7$ s would be twice the MHA value of $0.2g$.

## 25.4 Soil Liquefaction

Unlike many other construction materials, cohesionless soils such as sand possess negligible strength without effective confinement. The overall strength of an uncemented sand depends on particle interaction (interparticle friction and particle rearrangement), and these particle interaction forces depend on the effective confining stresses. Soil **liquefaction** is a phenomenon resulting when the pore water pressure (the water pressure in the pores between the soil grains) increases, thereby reducing the effective confining stress and hence the strength of the soil. Seed and Idriss [1982] present this qualitative explanation of soil liquefaction:

If a saturated sand is subjected to ground vibrations, it tends to compact and decrease in volume; if drainage is unable to occur, the tendency to decrease in volume results in an increase in pore water pressure, and if the pore water pressure builds up to the point at which it is equal to the overburden pressure, the effective stress becomes zero, the sand loses its strength completely, and it develops a liquefied state.

If the strength of the ground underlying a structure reduces below that required to support the overlying structure, excessive structural movements can occur and damage the structure. The pore water pressure in the liquefied soil may be sufficient to cause the liquefied soil to flow up through the overlying material to the ground surface producing sand boils, lateral spreading, and ground breakage. This dramatic seismic response of a saturated, loose sand deposit can pose obvious hazards to constructed facilities, and the potential for soil liquefaction should be assessed in seismic regions where such soil deposits exist.

An example of the structural damage that can result from soil liquefaction is shown in Fig. 25.7. The Marine Research Facility at Moss Landing, California was a group of modern one-and two-story structures founded on concrete slabs. This facility was destroyed beyond repair by foundation displacements as a result of liquefaction of the foundation soils during the 1989 Loma Prieta earthquake [Seed et al., 1990]. The facility settled a meter or two and lateral spreading of the structure "floating" on the liquefied soil below the slab foundation stretched the facility by 2 m, literally pulling it apart.

Engineering procedures for evaluating liquefaction potential have developed rapidly in the past twenty years, and a well-accepted approach is the Seed and Idriss [1982] simplified procedure for evaluating soil liquefaction potential. The average cyclic shear stress imparted by the earthquake in the upper 12 m of a soil deposit can be estimated using the equation developed by Seed and Idriss [1982]:

$$(\tau/\sigma_0')_d \approx 0.65 \cdot \mathrm{MHA}/g \cdot \sigma_0/\sigma_0' \cdot r_d \tag{25.2}$$

where

$(\tau/\sigma_0')_d$ = average cyclic stress ratio developed during the earthquake
MHA = maximum horizontal acceleration at the ground surface
$g$ = acceleration of gravity
$\sigma_0$ = total stress at depth of interest
$\sigma_0'$ = effective stress (total stress minus pore water pressure) at depth
$r_d$ = reduction in acceleration with depth ($r_d \approx 1 - 0.008 \cdot$ depth, m)

For a magnitude ($M_s$) 7.5 event at a level ground site, the cyclic stress ratio required to induce liquefaction, $(\tau/\sigma_0')_l$, of the saturated sand deposit can be estimated using the empirically based standard penetration test (SPT) correlations developed by Seed et al. [1985]. The SPT blowcount (the number of hammer blows required to drive a standard sampling device 1 foot into the soil deposit) provides an index of the *in situ* state of a sand deposit, and especially of its relative density. Field measured SPT

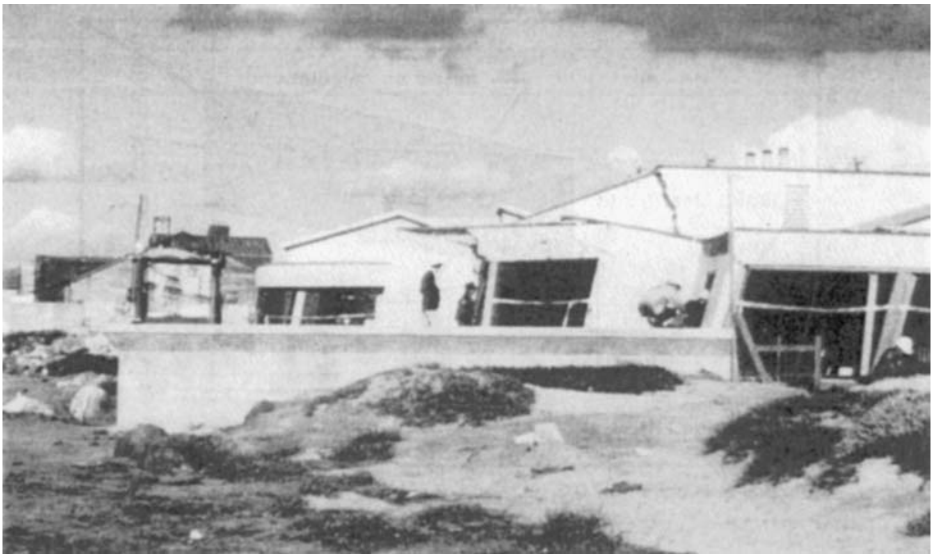

**FIGURE 25.7** Liquefaction-induced damage of the Marina Research Facility at Moss Landing, California, caused by the 1989 Loma Prieta earthquake (after Seed, R. B., Dickenson, S. E., Riemer, M. F., Bray, J. D., Sitar, N., Mitchell, J. K., Idriss, I. M., Kayen, R. E., Kropp, A., Harder, L. F., and Power, M. S. 1990. Preliminary Report on the Principal Geotechnical Aspects of the October 17, 1989 Loma Prieta Earthquake. Earthquake Engineering Research Center, Report No. UCB/EERC-90/05, University of California).

blowcount numbers are corrected to account for overburden pressure, hammer efficiency, saturated silt, and other factors. A loose sand deposit will generally have low SPT blowcount numbers (4–10) and a dense sand deposit will generally have high SPT blowcount numbers (30–50). Moreover, changes in factors that tend to increase the cyclic loading resistance of a deposit similarly increase the SPT blowcount. Hence, the cyclic stress required to induce soil liquefaction can be related to the soil deposit's penetration resistance. Well-documented sites where soil deposits did or did not liquefy during earthquake strong shaking were used to develop the correlation shown in Fig. 25.8. Correction factors can be applied to the $(\tau/\sigma_0')_l$ versus SPT correlation presented in Fig. 25.8 to account for earthquake magnitude, greater depths, and sloping ground [see Seed and Harder, 1990].

Finally, the liquefaction susceptibility of a saturated sand deposit can be assessed by comparing the cyclic stress ratio required to induce liquefaction, $(\tau/\sigma_0')_l$, with the average cyclic stress ratio developed during the earthquake, $(\tau/\sigma_0')_d$. A reasonably conservative factor of safety should be employed ($\approx 1.5$) because of the severe consequences of soil liquefaction.

## Illustrative Soil Liquefaction Problem

### Problem 25.2

Evaluate the liquefaction susceptibility of the soil deposit shown in Fig. 25.4.

***Soil Liquefaction***

At this site, MHA $\approx 0.2g$ (see Problem 25.1). At a depth of 5 m, $\sigma_0 = \rho_t \cdot g \cdot z = (2.0\ \text{Mg/m}^3)(9.81\ \text{m/s}^2)(5\ \text{m}) = 98$ kPa; $\sigma_0' = \sigma_0 - \gamma_w \cdot z_w = 98\ \text{kPa} - (1\ \text{Mg/m}^3)(9.81\ \text{m/s}^2)(3\ \text{m}) = 68$ kPa; and $r_d \approx 1.0 - 0.008(5m) = 0.96$. Hence, using Eq. (25.2), the average cyclic stress ratio developed during the earthquake is

$$(\tau/\sigma_0')_d \approx 0.65 \cdot (0.2g/g) \cdot \frac{98\ \text{kPa}}{68\ \text{kPa}} \cdot 0.96 = 0.18 \tag{25.3}$$

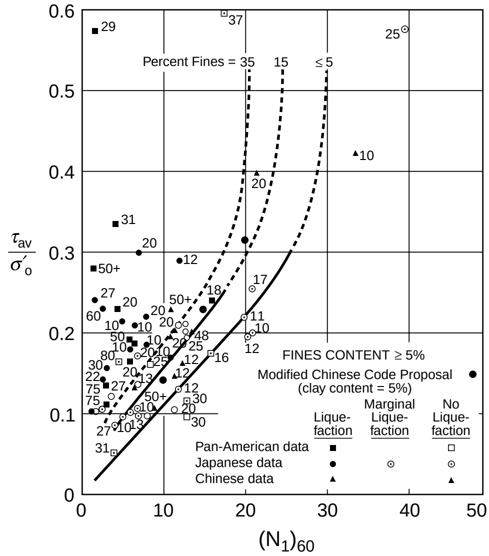


**FIGURE 25.8** Relationship between stress ratios causing liquefaction and $(N_1)_{60}$-values for silty sands for $M_s = 7\frac{1}{2}$ earthquakes (after Seed, H. B., Tokimatsu, K., Harder, L. F., and Chung, R. M. 1985. Influence of SPT Procedures in Soil Liquefaction Resistance Evaluations. *Journal of the Geotechnical Engineering Division,* ASCE. (111) 12:1425–1445).

The corrected penetration resistance of the sand at a depth of 5 m is around 10, and using Fig. 25.8, for a clean sand with less than 5% fines, $(\tau/\sigma'_0)_l \approx 0.11$.

The factor of safety (FS) against liquefaction is then

$$FS = (\tau/\sigma'_0)_l/(\tau/\sigma'_0)_d = 0.11/0.18 = 0.6 \tag{25.4}$$

Since the factor of safety against liquefaction is less than 1.0, the potential for soil liquefaction at the site is judged to be high. Modern ground improvement techniques (e.g., dynamic compaction) may be used to densify a particular soil deposit to increase its liquefaction resistance and obtain satisfactory performance of the building's foundation material during earthquake strong shaking.

## 25.5 Seismic Slope Stability

Considerable attention has been focused over the last few decades on developing procedures to analyze the seismic performance of earth embankments [e.g., Newmark, 1965; Seed, 1979; Marcuson et al., 1992]. The first issue that must be addressed is an evaluation of the potential of the materials comprising the earth structure to lose significant strength under cyclic earthquake loading. Saturated cohesionless materials (gravels, sands, and nonplastic silts) that are in a loose state are prime candidates for liquefaction and hence significant strength loss. Experience has shown that cohesionless materials placed by the hydraulic fill method are especially vulnerable to severe strength loss as a result of strong shaking. A modified version of the Seed and Idriss [1982] simplified method has been employed to evaluate the liquefaction potential of cohesionless soils in earth slopes and dams [see Seed and Harder, 1990]. Certain types of clayey materials have also been shown to lose significant strength as a result of cyclic loading. If clayey materials have a small percentage of clay-sized particles, low liquid limits, and high water contents, the material's cyclic loading characteristics should be determined by cyclic laboratory testing [Seed and Idriss, 1982].

The potentially catastrophic consequences of an earth embankment material that undergoes severe strength loss during earthquake shaking is demonstrated by the near failure of the Lower San Fernando

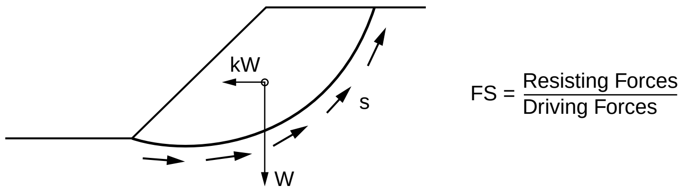


**FIGURE 25.9** Pseudostatic slope stability analysis.

dam as a result of the 1971 San Fernando earthquake [Seed et al., 1975]. The center and upstream sections of the dam slid into the reservoir because a large section within the dam liquefied. The slide movement left only 1.5 m of earth fill above the reservoir level. Fortunately, the reservoir level was 11 m below the original crest at the time of the earthquake. Still, because of the precarious condition of the dam after the main shock, 80,000 people living downstream of the dam were ordered to evacuate until the reservoir could be lowered to a safe elevation.

Surveys of earth dam performance during earthquakes suggest that embankments constructed of materials that are not vulnerable to severe strength loss as a result of earthquake shaking (most well-compacted clayey materials, unsaturated cohesionless materials, and some dense saturated sands, gravels, and silts) generally perform well during earthquakes [Seed et al., 1978]. The embankment, however, may undergo some level of permanent deformation as a result of the earthquake shaking. With well-built earth embankments experiencing moderate earthquakes, the magnitude of permanent seismic deformations should be small, but marginally stable earth embankments experiencing major earthquakes may undergo large deformations that may jeopardize the structure's integrity. Simplified procedures have been developed to evaluate the potential for seismic instability and seismically induced permanent deformations [e.g., Seed, 1979; Makdisi and Seed, 1978], and these procedures can be used to evaluate the seismic performance of earthen structures and natural slopes.

In pseudostatic slope stability analyses, a factor of safety against failure is computed using a static limit equilibrium stability procedure in which a pseudostatic, horizontal inertial force, which represents the destabilizing effects of the earthquake, is applied to the potential sliding mass. The horizontal inertial force is expressed as the product of a seismic coefficient, $k$, and the weight, $W$, of the potential sliding mass (Fig. 25.9). If the factor of safety approaches unity, the embankment is considered unsafe. Since the seismic coefficient designates the horizontal force to be used in the stability analysis, its selection is crucial. The selection of the seismic coefficient must be coordinated with the selection of the dynamic material strengths and minimum factor of safety, however, as these parameters work together to achieve a satisfactory design. For earth embankments, case histories are available which have guided the selection of these parameters. For example, Seed [1979] recommends using appropriate dynamic material strengths, a seismic coefficient of 0.15, and a minimum factor of safety of 1.15 to ensure that an embankment composed of materials that do not undergo severe strength loss performs satisfactorily during a major earthquake.

A significant limitation of the pseudostatic approach is that the horizontal force, representing the effects of an earthquake, is constant and acts in only one direction. With dynamically applied loads, the force may be applied for only a few tenths of a second before the direction of motion is reversed. The result of these transient forces will be a series of displacement pulses rather than complete failure of the slope. Normally, a certain amount of limiting displacement during an earthquake event is considered tolerable. Hence, if conservative strength properties are selected and the seismic coefficient represents the maximum disturbing force (i.e., maximum shear stress induced by the earthquake on the potential sliding surface; see Seed and Martin, 1966), a factor of safety of one is likely to ensure adequate seismic performance. Other conservative combinations of these parameters could be developed, but their use must be evaluated in the context that their use in analysis ensures a design that performs well during earthquakes (i.e., tolerable deformations).

Seismically induced permanent deformations are generally calculated using a Newmark-type procedure. The Newmark [1965] analysis assumes that relative slope movements would be initiated when the inertial force on a potential sliding mass was large enough to overcome the yield resistance along the slip surface, and these movements would stop when the inertial force decreased below the yield resistance and the velocities of the ground and sliding mass coincided. The yield acceleration is defined as the average acceleration producing a horizontal inertial force on a potential sliding mass which gives a factor of safety of one and can be calculated as the seismic coefficient in pseudostatic slope stability analyses that produces a safety factor of one. By integrating the equivalent average acceleration [see Bray et al., 1993] acting on the sliding surface in excess of this yield acceleration as a function of time, the displacement of the slide mass can be estimated. A commonly used procedure for calculating seismically induced permanent deformations has been developed by Franklin and Chang [1977] and computer programs are available [e.g., Pyke and Beikae, 1991]. Simplified chart solutions have been developed by Makdisi and Seed [1978] for earth embankments.

An emerging area of concern in many regions of the world is the seismic performance of waste fills. For example, recent U.S. federal regulations (40 CFR 258-USEPA 1991: Subtitle D) require that municipal solid waste landfills located in seismic impact zones be designed to resist earthquake hazards. Since these designated seismic impact zones encompass nearly half of the continental U.S., these regulations are having a pronounced impact on the design of new landfills and the lateral expansion of existing landfills. The results of a comprehensive study of the effects of the characteristics of the waste fill, subsurface soils, and earthquake ground motions are presented in Bray et al. [1993]. The investigators found that the seismic loading strongly depends on the dynamic properties and height of the waste fill. General design considerations regarding the seismic stability of solid waste landfills are discussed in Repetto et al. [1993].

## 25.6 Summary

Geotechnical earthquake engineering phenomena such as site-specific amplification, soil liquefaction, and seismic slope stability are important aspects of earthquake engineering, and these aspects must be adequately addressed in the development of sound earthquake-resistant designs. Seismic risk assessments of a facility, community, or region must incorporate engineering analyses that properly evaluate the potential hazards resulting from these phenomena. Deep soil deposits can amplify the underlying bedrock ground motions and produce intense levels of shaking at significant distances from the earthquake's epicenter. Under sufficient cyclic loading, loose, saturated sand deposits may suddenly liquefy, undergo severe strength loss, and fail as a foundation or dam material. Seismically induced permanent deformations of a landfill's liner system can jeopardize the integrity of the system and potentially release pollutants into the environment. Simplified empirical procedures employed to evaluate these hazards have been presented and they provide a starting point. The field of earthquake engineering is quite complex, however, and there are many opportunities for future research.

### Defining Terms

**Attenuation relationship —** Provides the value of an engineering parameter versus distance from the zone of energy release of an earthquake.

**Damping ratio —** An indication of the ability of a material to dissipate vibrational energy.

**Duration of strong shaking —** Duration of the earthquake record in which the intensity is sufficiently high to be of engineering importance (i.e., MHA $\geq 0.05g$).

**Fundamental period —** Period at which a structure tends to vibrate when allowed to vibrate freely without any external excitation.

**Liquefaction —** Phenomenon resulting when the pore-water pressure within saturated particulate material increases dramatically, resulting in a severe loss of strength.

**Magnitude —** Measure of the amount of energy released during an earthquake. Several magnitude scales exist (e.g., local magnitude, $M_L$, and moment magnitude, $M_w$).

**Maximum horizontal ground acceleration (MHA) —** Highest horizontal ground acceleration recorded at a free-field site (i.e., not in a structure) during an earthquake.

**Predominant period (Tp) —** Period at which most of the seismic energy is concentrated, often defined as the period at which the maximum spectral acceleration occurs.

**Response spectrum —** Displays maximum response induced by ground motions in damped single-degree-of-freedom structures of different fundamental periods.

**Shear wave velocity (Vs) —** Speed that shear waves travel through a medium. An indication of the dynamic stiffness of a material. Note that $G = \rho V_s^2$, where $G$ = shear modulus and $\rho$ = mass density.

## References


Algermissen, S. T., Perkins, D. M., Thenhous, P. C., Hanson, S. L., and Bender, B. L. 1991. Probabilistic earthquake acceleration and velocity maps for the United States and Puerto Rico. *U.S.G.S. Misc. Field Stud*. Map MF2120.

Allen and Hoshall. 1985. *An Assessment of Damage and Casualties*. Federal Emergency Management Agency Report, Sections V and XI.

Bray, J. D., Chameau, J. L., and Guha, S. 1992. Seismic response of deep stiff clay deposits. In *Proc. 1st Can. Symp. Geo. Nat. Hazards,* Vancouver, BC, May 6–9, pp. 167–174.

Bray, J. D., Repetto, P. C., Angello, A. J., and Byrne, R. J. 1993. An overview of seismic design issues for solid waste landfills. In *Proc. Geosynth. Res. Inst. Conf.,* Drexel University, Philadelphia, December.

Building Officials & Code Administrators International, Inc. 1992. *National Building Code*. Country Club Hills, IL.

Franklin, A. G., and Chang, F. K. 1977. Earthquake resistance of earth and rockfill dams. Misc. Pap. S-71-17, U.S. Army Waterways Experiment Station, Vicksburg, MS, November, 1977.

Gutenberg, B., and Richer, C. F. 1956. Earthquake magnitude, intensity, energy and acceleration. *B. Seism. Soc. Am*. 46(2):143–145.

Hanks, T. C., and Kanamori, H. 1979. A moment magnitude scale. *J. Geophys. Res*. 82:2981–2987.

Heaton, T. H., Tajima, F., and Mori, A. W. 1982. *Estimating Ground Motions Using Recorded Accelerograms*. Report by Dames & Moore to Exxon Production Res. Co., Houston.

Hopper, M. G., ed. 1985. *Estimation of Earthquake Effects Associated with Large Earthquakes in the New Madrid Seismic Zone*. U.S. Geological Survey Open-File Report 85-457.

Hough, S. E., Friberg, P. A., Busby, R., Field, E. F., Jacob, K. H., and Borcherdt, R. D. 1990. Sediment-induced amplification and the collapse of the Nimitz Freeway, *Nature.* 344:853–855.

Hynes, M. E., and Franklin, A. G. 1984. Rationalizing the seismic coefficient method. Misc. Pap. GL-84-13. U.S. Army Engineer WES, Vicksburg, MS.

Idriss, I. M. 1985. Evaluating seismic risk in engineering practice. In *Proc. 11th Int. Conf. Soil Mech. Found. Eng*. August 12–16, 1985, San Francisco, Vol. I, pp. 255–320.

Idriss, I. M. 1991. Earthquake ground motions at soft soil sites. In *Proc. 2nd Int. Conf. Recent Adv. Geo. Eng. Soil Dyn*. March 11–15, St. Louis, pp. 2265–2272.

Idriss, I. M., and Sun, J. I. 1992. *User's Manual for SHAKE91 — A Computer Program for Conducting Equivalent Linear Seismic Response Analyses of Horizontally Layered Soil Deposits*. Center for Geotechnical Modeling, Dept. of Civil and Environ. Eng., University of California, Davis, November.

International Conference of Building Officials. 1991. *Uniform Building Code*. Whittier, CA.

Joyner, W. B., and Boore, D. M. 1988. Measurement characteristics and prediction of strong ground motion: state-of-the-art reports. In *Proc. Spec. Conf. Earthquake Eng. Soil Dyn. II,* ASCE, pp. 43–102.

Makdisi, F. I., and Seed, H. B. 1978. Simplified procedure for estimating dam and embankment earthquake-induced deformation. *J. Geotech. Eng., ASCE*. 104(7):849–867.

Marcuson, W. F., III, Hynes, M. E., and Franklin, A. G. 1992. Seismic stability and permanent deformation analyses: The last twenty-five years. In *Proc. ASCE Spec. Conf. Stability and Performance of Slopes and Embankments — II*. Berkeley, CA, June 28–July 1, pp. 552–592.

Newmark, N. M. 1965. Effects of earthquakes on dams and embankments. *Geotechnique*. 15(2):139–160.

Nuttli, O. W. 1982. Advances in seismicity and tectonics. In *Proc. 3rd Int. Earthquake Microzonation Conf.* Vol. I, pp. 3–24.

Nuttli, O. W., and Herrmann, R. B. 1984. Ground motion of Mississippi Valley earthquakes. *J. Tech. Top. Civ. Eng., ASCE*. 110:(54–69).

Nuttli, O. W. 1987. The Current and Projected State-of-Knowledge on Earthquake Hazards. Unpublished report presented in St. Louis, MO.

Pyke, R., and Beikae, M. 1991. TNMN. Taga Engineering Software Services, Lafayette, CA.

Repetto, P. C., Bray, J. D., Byrne, R. J., and Augello, A. J. 1993. Seismic design of landfills. In *Proc. 13th Cent. Pa. Geotech. Semin.,* Penn. DOT & ASCE, April 12–14.

Richter, C. F. 1935. An instrumental earthquake scale. *B. Seism. Soc. Am*. 25(1):1–32.

Richter, C. F. 1958. *Elementary Seismology.* W. H. Freeman, San Francisco.

Seed, H. B., and Martin, G. R. 1966. The seismic coefficient in earth dam design. *J. Soil Mech. Found., ASCE*. 92(3):25–58.

Seed, H. B., Lee, K. L., Idriss, I. M., and Makdisi, F. I. 1975. The slides in the San Fernando dams during the earthquake of February 9, 1971. *J. Geotech. Eng., ASCE*. 101(7):889–911.

Seed, H. B., Makdisi, F. I., and DeAlba, P. 1978. Performance of earth dams during earthquakes. *J. Geotech. Eng., ASCE*. 104(7):967–994.

Seed, H. B. 1979. Considerations in the earthquake-resistant design of earth and rockfill dams. *Geotechnique*. 29(3):215–263.

Seed, H. B., and Idriss, I. M. 1982. Ground motions and soil liquefaction during earthquakes. Monograph, Earthquake Engineering Research Institute, Berkeley, CA.

Seed, H. B. 1983. Earthquake-resistant design of earth dams. Paper presented at ASCE National Convention, Philadelphia, May 16–20, pp. 41–64.

Seed H. B., Wong, R. T., Idriss, I. M., and Tokimatsu, K. 1984. Moduli and damping factors for dynamic analyses of cohesionless soils. Earthquake Engineering Research Center, Report No. UCB/EERC-84/14, University of California, Berkeley, October.

Seed, H. B., Tokimatsu, K., Harder, L. F., and Chung, R. M. 1985. Influence of SPT procedures in soil liquefaction resistance evaluations. *J. Geotech. Eng., ASCE*. (111)12:1425–1445.

Seed, H. B., Romo, M. P., Sun, J., Jaime, A., and Lysmer, J. 1987. Relationships between soil conditions and earthquake ground motions in Mexico City in the earthquake of Sept. 19, 1985. Earthquake Engineering Research Center, Report No. UCB/EERC-87/15, University of California, Berkeley.

Seed, R. B., Dickenson, S. E., Riemer, M. F., Bray, J. D., Sitar, N., Mitchell, J. K., Idriss, I. M., Kayen, R. E., Kropp, A., Harder, L. F., and Power, M. S. 1990. Preliminary report on the principal geotechnical aspects of the October 17, 1989 Loma Prieta earthquake. Earthquake Engineering Research Center, Report No. UCB/EERC-90/05, University of California.

Seed, R. B., and Harder, Jr., L. F. 1990. SPT-based analysis of cyclic pore pressure generation and undrained residual strength. *H. Bolton Seed Memorial Symp.,* Vol. II, May, pp. 351–376.

Seed, R. B., and Bonaparte, R. 1992. Seismic analysis and design of lined waste fills: Current practice. In *Proc. ASCE Spec. Conf. Stability and Performance of Slopes and Embankments — II*. Berkeley, CA, June 28–July 1, pp. 1521–1545.

Southern Building Code Congress International. 1992. *Standard Building Code*. Birmingham, Alabama.

United States Code of Federal Regulations, Title 40. 1991. Protection of the Environment, Part 258, *Solid Waste Disposal Facility Criteria*.

Vucetic, M., and Dobry, R. 1991. Effect of soil plasticity on cyclic response. *J. Geotech. Eng., ASCE*. 117(1):89–107.

## Further Information

"Ground Motions and Soil Liquefaction during Earthquakes" by Seed and Idriss [1982] provides an excellent overview of site-specific amplification and soil liquefaction. Seed and Harder [1990] present an up-to-date discussion of soil liquefaction. "Evaluating Seismic Risk in Engineering Practice" by Idriss [1985] provides an excellent discussion of seismicity and geotechnical earthquake engineering. Seismic stability considerations in earth dam design are presented in "Considerations in the Earthquake-Resistant Design of Earth and Rockfill Dams" by Seed [1979]. Seismic design issues concerning solid waste landfills are presented in Bray et al. [1993].